RESEARCH BRIEF

The Vigorous Immune Microenvironment of Microsatellite Instable Colon Cancer Is Balanced by Multiple Counter-Inhibitory Checkpoints

Nicolas J. Llosa[1], Michael Cruise[2], Ada Tam[3], Elizabeth C. Wicks[4], Elizabeth M. Hechenbleikner[4], Janis M. Taube[2], Richard L. Blosser[3], Hongni Fan[1], Hao Wang[5], Brandon S. Luber[5], Ming Zhang[6], Nickolas Papadopoulos[6], Kenneth W. Kinzler[6], Bert Vogelstein[6], Cynthia L. Sears[1,7], Robert A. Anders[2], Drew M. Pardoll[1,2,7,8], and Franck Housseau[1]

ABSTRACT

We examined the immune microenvironment of primary colorectal cancer using immunohistochemistry, laser capture microdissection/qRT-PCR, flow cytometry, and functional analysis of tumor-infiltrating lymphocytes. A subset of colorectal cancer displayed high infiltration with activated $CD8^+$ cytotoxic T lymphocyte (CTL) as well as activated Th1 cells characterized by IFNγ production and the Th1 transcription factor TBET. Parallel analysis of tumor genotypes revealed that virtually all of the tumors with this active Th1/CTL microenvironment had defects in mismatch repair, as evidenced by microsatellite instability (MSI). Counterbalancing this active Th1/CTL microenvironment, MSI tumors selectively demonstrated highly upregulated expression of multiple immune checkpoints, including five—PD-1, PD-L1, CTLA-4, LAG-3, and IDO—currently being targeted clinically with inhibitors. These findings link tumor genotype with the immune microenvironment, and explain why MSI tumors are not naturally eliminated despite a hostile Th1/CTL microenvironment. They further suggest that blockade of specific checkpoints may be selectively efficacious in the MSI subset of colorectal cancer.

SIGNIFICANCE: The findings reported in this article are the first to demonstrate a link between a genetically defined subtype of cancer and its corresponding expression of immune checkpoints in the tumor microenvironment. The mismatch repair–defective subset of colorectal cancer selectively upregulates at least five checkpoint molecules that are targets of inhibitors currently being clinically tested. *Cancer Discov; 5(1); 43–51. ©2014 AACR.*

See related commentary by Xiao and Freeman, p. 16.

[1]Department of Oncology, Sidney Kimmel Comprehensive Cancer Center, Johns Hopkins University, Baltimore, Maryland. [2]Department of Pathology, Johns Hopkins University, Baltimore, Maryland. [3]Flow Cytometry Core, Sidney Kimmel Comprehensive Cancer Center, Johns Hopkins University, Baltimore, Maryland. [4]Department of Surgery, Johns Hopkins University, Baltimore, Maryland. [5]Department of Oncology Biostatistics and Bioinformatics, Sidney Kimmel Comprehensive Cancer Center, Johns Hopkins University, Baltimore, Maryland. [6]Ludwig Center for Cancer Genetics and Therapeutics, Howard Hughes Medical Institute, and the Sidney Kimmel Comprehensive Cancer Center, Johns Hopkins University, Baltimore, Maryland. [7]Department of Medicine, Johns Hopkins University, Baltimore, Maryland. [8]Department of Molecular Biology and Genetics, Sidney Kimmel Comprehensive Cancer Center, Johns Hopkins University, Baltimore, Maryland.

Note: Supplementary data for this article are available at Cancer Discovery Online (http://cancerdiscovery.aacrjournals.org/).

Current address for M. Cruise: Department of Anatomic Pathology, Cleveland Clinic, Cleveland, Ohio.

Corresponding Authors: Franck Housseau, Sidney Kimmel Comprehensive Cancer Center, Johns Hopkins University School of Medicine, CRB-I/Suite 440, 1650 Orleans Street, Baltimore, MD 21287. Phone: 410-955-7866; Fax: 410-614-0549; E-mail: fhousse1@jhmi.edu; and Drew M. Pardoll, Dpardol1@jhmi.edu

doi: 10.1158/2159-8290.CD-14-0863

INTRODUCTION

An increasing body of research has revealed that the immune microenvironment of cancer is unique and complex; indeed, tumors can be viewed as distinct immunologic organs. Pathologists have long recognized the diversity of immune infiltration into tumors, invoking terms such as "lymphocyte poor" and "inflammatory." For some cancer types, it is becoming clear that simple quantitation of lymphocyte infiltration has prognostic significance, suggesting that lymphocyte infiltration is not passive but may actively promote or inhibit tumor growth (1). In the case of colorectal cancer, Galon and colleagues (2) demonstrated that levels of lymphocyte infiltration into primary tumors represented a strong independent predictor of relapse and overall survival, with high lymphocyte infiltration being a positive prognostic factor. Using expression profiling of colorectal cancers, they further defined the relevance of specific immune signatures, demonstrating that T helper 1 cells (Th1)–type, IFNγ-dominant immune profiles signified an improved prognosis, whereas Th17–type, IL17-dominant immune profiles signified a poor prognosis (3). These findings are in concordance with multiple studies in murine models demonstrating that Th1/cytotoxic T lymphocyte (CTL)–dominant immune responses are antitumorigenic (4), whereas Th17-dominant responses are typically procarcinogenic (5).

The relevance of molecular regulation of lymphocyte function in the tumor microenvironment (TME) has been further highlighted by the emerging clinical experience in treatment of cancer with antibody blockade of the PD-1 pathway. Anti–PD-1 and anti–PD-L1 antibodies have been demonstrated to induce significant durable tumor regressions in patients with melanoma, renal cancer, and non–small cell lung cancer (6–9). The finding that expression of PD-L1 in tumor biopsies is a predictor of response to PD-1 pathway–blocking antibodies (6) supports conclusions from murine studies that this pathway plays a major role in blocking antitumor immune responses directly within the TME (10). With increasing efforts to develop antibody blockers of multiple additional immune-inhibitory ligands and receptors (termed checkpoints) for cancer immunotherapy, understanding the expression patterns and functions of these molecules in the context of the TME will be critical in selecting patient populations most likely to benefit from their application (11). In contrast to melanoma, renal cancer, and lung cancer, colorectal cancer cohorts demonstrated a very low response rate to PD-1 or PD-L1 blockade and have been considered a nonresponding histology to the PD-1 pathway blockade (6–8). However, there was an insufficient number of patients to potentially define subsets of colorectal cancer that might be more amenable to checkpoint blockade.

With these considerations in mind, we have undertaken a comprehensive analysis of the immune microenvironment of colorectal cancer, using a combination of immunohistochemistry (IHC), laser capture microdissection combined with quantitative reverse transcription PCR (LCM/qRT-PCR), multiparameter flow cytometry (MFC), and functional analysis of purified tumor-infiltrating lymphocytes (TIL) from a large set of surgically resected primary colorectal cancer. These analyses revealed, in an unbiased fashion, that a subset of colorectal cancer possesses a highly activated Th1- and CTL-rich microenvironment. Through concomitant genetic analysis, we found that this subset of tumors harbored microsatellite instability (MSI), indicating that they were mismatch repair–deficient (12). This finding was in accordance with numerous prior studies indicating that MSI tumors are highly infiltrated with T cells including CTLs (13–16). How could tumors persist in this hostile microenvironment? To find out, we carried out an extensive investigation of the regulatory factors operative in this microenvironment. We found that there was a dramatic overexpression of immune checkpoint–related proteins in the microenvironment of MSI tumors, thus explaining a long-standing enigma and suggesting that immunotherapeutic interventions involving checkpoint blockade might be selectively effective in this important subset of cancers. On the basis of these findings, clinical trials have been initiated to test PD-1 blockade in patients with colorectal cancer identified as MSI.

RESULTS

We began our analysis of primary sporadic colorectal cancer by performing quantitative IHC for standard T-cell subsets using antibodies to CD3, CD4, CD8, and Foxp3. We distinguished three compartments: true TIL representing lymphocytes intercalated within the glandular or medullary epithelial component of the tumor, T cells in the tumor stroma surrounding the epithelial component of the tumor, and the invasive front where the tumor invades into the lamina propria (Supplementary Fig. S1). Infiltration by these T-cell types in each of the compartments was quantitated numerically by blinded analysis of 5 high-power fields (hpf; 0.0028 mm^2/hpf) and displayed as average number of stained cells per hpf. We found a subset of tumors (roughly 20%) that had large infiltrates of total ($CD3^+$ T cells) as well as $CD4^+$ and $CD8^+$ T cells in all three compartments, with $CD8^+$ T cells the most dramatically increased. We wondered whether this subset of tumors was MSI, given prior studies indicating lymphocyte infiltrations in such tumors (13–16). Indeed, analysis of microsatellites showed that nearly all of the tumors with the infiltrates were MSI. We therefore focused on differences between tumors harboring MSI versus microsatellite stability (MSS; Supplementary Table S1) for the in-depth analysis of the immune TME of colorectal cancer.

Figure 1A and B show typical examples of IHC staining, and Fig. 1C shows the quantitative analyses demonstrating statistical differences between MSI and MSS tumors for the total $CD3^+$ T cells and $CD4^+$ T cells among TIL and invasive front as well as $CD8^+$ T cells among all three compartments. Although it did not reach statistical significance in tumor stroma and the invasive front, we observed higher $Foxp3^+$ cell infiltrates, representative of regulatory T cells (Treg), in MSI compared with MSS tumors. Of note, a single outlier included in our MSS cohort displayed a high infiltration of each T-cell subset, similar in range to the one of MSI tumors (Fig. 1C and Supplementary Figs. S2 and S3A).

We further explored the nature of the T-cell infiltrates by performing LCM on MSI and MSS tumors, separately dissecting the TIL, stroma, and invasive front compartments (Supplementary Fig. S1) and then performed qRT-PCR (Fig. 2A–C)

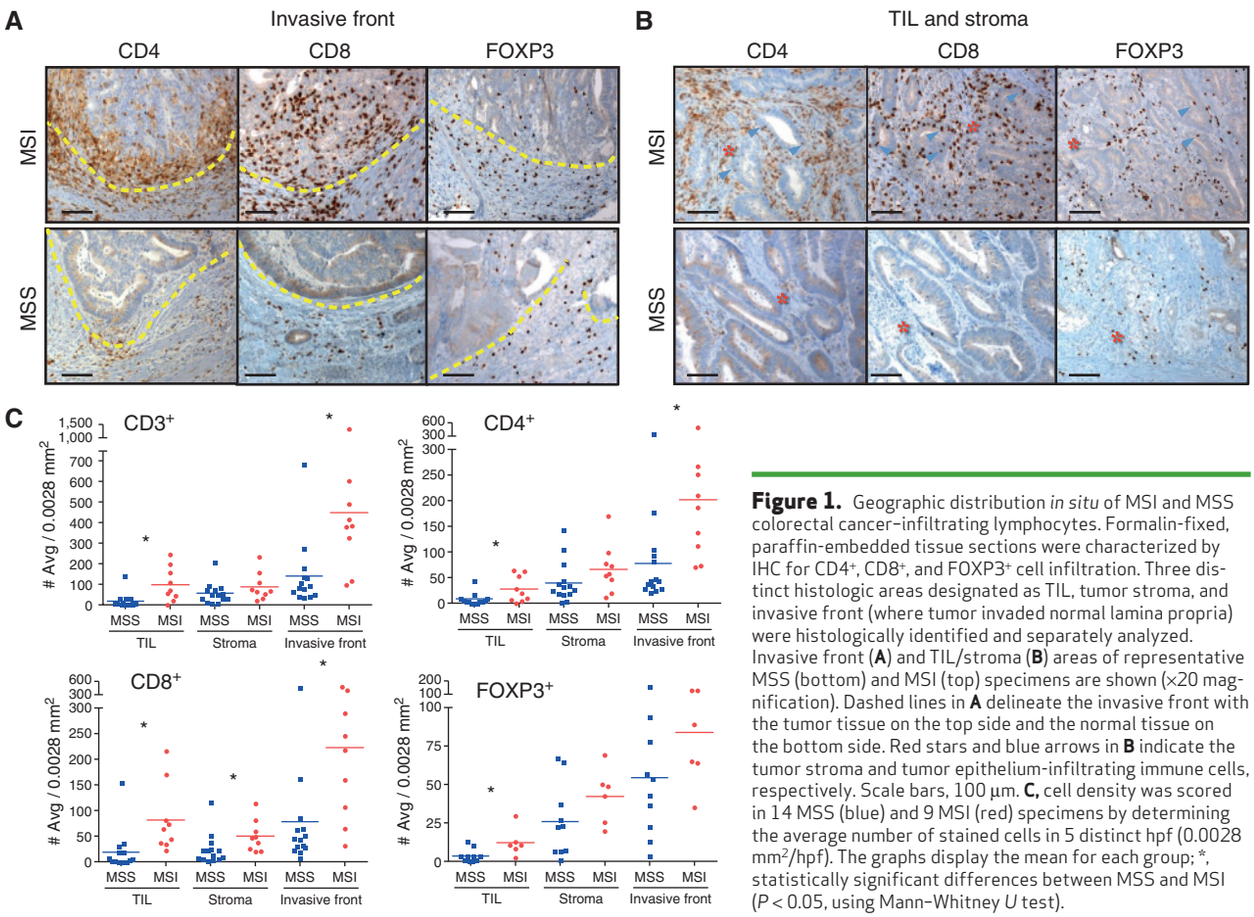

Figure 1. Geographic distribution *in situ* of MSI and MSS colorectal cancer–infiltrating lymphocytes. Formalin-fixed, paraffin-embedded tissue sections were characterized by IHC for $CD4^+$, $CD8^+$, and $FOXP3^+$ cell infiltration. Three distinct histologic areas designated as TIL, tumor stroma, and invasive front (where tumor invaded normal lamina propria) were histologically identified and separately analyzed. Invasive front (**A**) and TIL/stroma (**B**) areas of representative MSS (bottom) and MSI (top) specimens are shown (×20 magnification). Dashed lines in **A** delineate the invasive front with the tumor tissue on the top side and the normal tissue on the bottom side. Red stars and blue arrows in **B** indicate the tumor stroma and tumor epithelium-infiltrating immune cells, respectively. Scale bars, 100 μm. **C,** cell density was scored in 14 MSS (blue) and 9 MSI (red) specimens by determining the average number of stained cells in 5 distinct hpf (0.0028 mm^2/hpf). The graphs display the mean for each group; *, statistically significant differences between MSS and MSI ($P < 0.05$, using Mann–Whitney *U* test).

for selected genes encoding signature T-cell cytokines as well as core transcription factors for each of the three major Th subsets, Th1/Tc1 (type I CTL; *TBX21* and *IFNG* are common to Th1 and Tc1), Th2, and Th17. We additionally analyzed genes associated with CTL and Treg and also general inflammatory cytokines. Finally, we analyzed expression of genes encoding both coinhibitory membrane ligands and receptors (commonly termed checkpoints) and metabolic enzymes that have been shown to regulate lymphocyte activity; these serve feedback-inhibitory functions in normal physiology but can represent important mechanisms of adaptive immune resistance by tumors in the face of an endogenous antitumor T-cell repertoire (11).

We found that the expression of the gene encoding IFNγ (*IFNG*), the canonical Th1/Tc1 cytokine, is higher in all three compartments of MSI compared with MSS tumors (Fig. 2A–C; the differences reach statistical significance in the TIL and invasive front areas with Wilcoxon test $P = 0.041$ for both). The expression of *TBX21* encoding TBET, the Th1/Tc1 canonical transcription factor, is similarly increased in MSI tumors, though differences did not reach statistical significance among the cohort analyzed. The *CD8A* gene, mainly expressed by CTLs, is highly differentially expressed in the TIL regions of MSI relative to MSS tumors (Fig. 2A; $P = 0.004$), in concordance with significantly higher CD8 infiltration observed by IHC (Fig. 1C). In marked contrast to Th1 and CTL genes, expression of Th17 genes is virtually identical between MSI and MSS tumors for all compartments. IL13 and IL4 (the canonical Th2-type cytokines) were undetectable in most of the MSI and MSS samples for each of the TME regions analyzed, and GATA3 (Th2 transcription factor) expression was not different between MSS and MSI (data not shown). Treg-associated genes, including *FOXP3*, were similar between MSI and MSS tumors. Gene group comparison analysis using the Wilcoxon–Mann–Whitney permutation test confirms that Th1/Tc1 (*TBX21* and *IFNG*) and CTL (*CD8A*, *GZMB*, *PRF1*, and *IL21*) groups but not the Th17 (*RORC*, *IL17A*, and *IL23*) group show statistical differences in their representation between TIL compartments of MSI and MSS colorectal cancer (Fig. 2D). In summary, MSI tumors have a selective Th1 and CTL infiltration and activation relative to MSS tumors. The highest value for *IFNG* and *TBX21* expression in TIL from a single MSS sample (detailed in Supplementary Fig. S3B) represents the same outlier observed in the quantitative analysis of CD4 and CD8 TIL infiltration from Fig. 1C. Among genes encoding inflammatory cytokines, *IL18*, which is generally associated with Th1 responses and selectively promotes IFNγ production by T cells, is more highly expressed in MSI tumors in all three compartments ($P < 0.05$), whereas genes encoding IL1 and IL6, which selectively promote Th17 responses, are not (Fig. 2A–C). The expression of *PTGS2* (encoding COX2), *IL12A* (encoding IL12p35), and *TNF* (encoding TNFα) did not differ between MSS and MSI specimens.

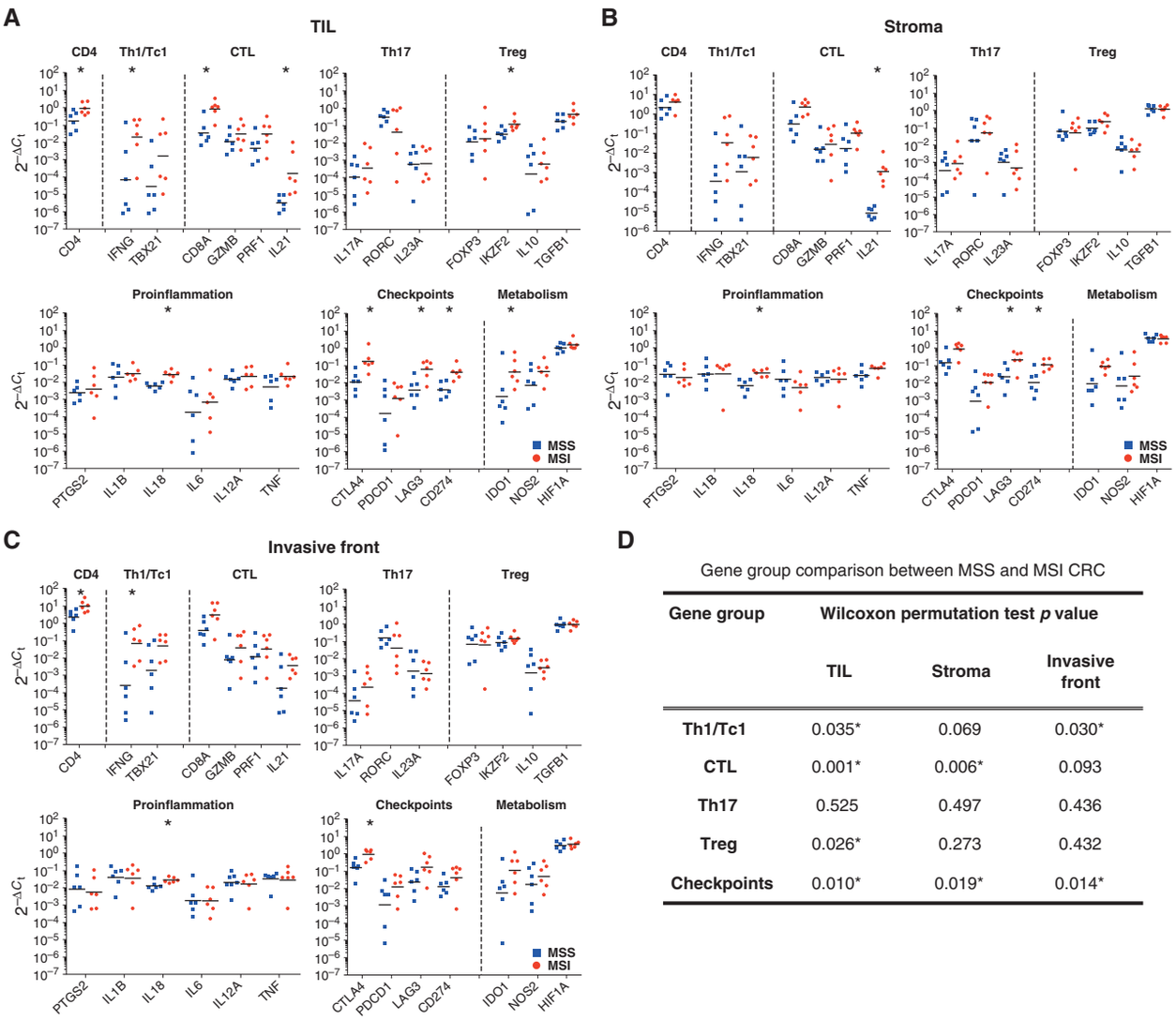

Gene group	Wilcoxon permutation test *p* value		
	TIL	Stroma	Invasive front
Th1/Tc1	0.035*	0.069	0.030*
CTL	0.001*	0.006*	0.093
Th17	0.525	0.497	0.436
Treg	0.026*	0.273	0.432
Checkpoints	0.010*	0.019*	0.014*

Figure 2. Th1 and CTL-based immune signature and elevated checkpoint expression in MSI colorectal cancer. RNA was extracted from tissue samples laser-microdissected representing TIL in tumor nests (**A**), stroma surrounding tumor (**B**), and invasive front (**C**) areas of MSS (blue squares) and MSI (red circles) colorectal cancer specimens. Immune-related gene expression profiles were assessed using TaqMan-based qRT-PCR for selected genes. Sets of genes were defined by functional relevance (Th1/Tc1, CTL, Th17, Treg, proinflammation, immune checkpoints, and metabolism). The *Y*-axis represents an arbitrary unit of expression $2^{-\Delta Ct}$, ΔC_t representing cycle threshold (C_t) of the gene of interest normalized by C_t of ubiquitous genes (*GUSB* and *GAPDH*). The graphs display the geometric means. Their differential representation between MSS and MSI specimens was analyzed using adjusted Wilcoxon–Mann–Whitney test as described in Methods. *, Wilcoxon $P < 0.05$. **D,** gene group comparison in TIL, tumor stroma, and invasive front areas between MSS and MSI specimens. Permutation test results based on the maximum Wilcoxon–Mann–Whitney test statistic within the gene groups Th1/Tc1, CTL, Th17, and immune checkpoints. *, statistically significant differences between MSS and MSI ($P < 0.05$).

We next analyzed the expression of genes encoding checkpoint receptors. We found that all three of the clinically targeted checkpoint receptors—CTLA-4 (*CTLA4*), PD-1 (*PDCD1*), and LAG-3 (*LAG3*)—were expressed at considerably higher levels in MSI compared with MSS tumors ($P < 0.05$ in all compartments for *CTLA4*, in TILs and the invasive front for *LAG3*; $P > 0.05$ in all compartments for *PDCD1*). The gene encoding PD-L1 (*CD274*), a major IFNγ-inducible PD-1 ligand expressed in the epithelial cells of many solid tumors (17), was unexpectedly expressed in TILs and stroma of MSI tumors (Wilcoxon test *P* values are 0.009 and 0.015, respectively; Fig. 2A and B). Among inhibitory metabolic enzymes, the IFNγ-induced gene encoding indolamine 2′3′-dioxygenase (IDO), which metabolizes tryptophan to kynurenine, demonstrates significantly higher expression in TILs of MSI tumors ($P = 0.041$; Fig. 2A). In contrast, arginase-1 (ARG1), a myeloid enzyme induced by the Th2 cytokines IL4 and IL13 and upregulated in M2 macrophages, was generally not detectable in either MSI or MSS tumors (data not shown). Thus, along with the Th1 and CTL genes, multiple immune-inhibitory genes, including a number that are IFNγ-induced, are preferentially expressed in the TILs and stroma of MSI tumors. Of note, these results reflect

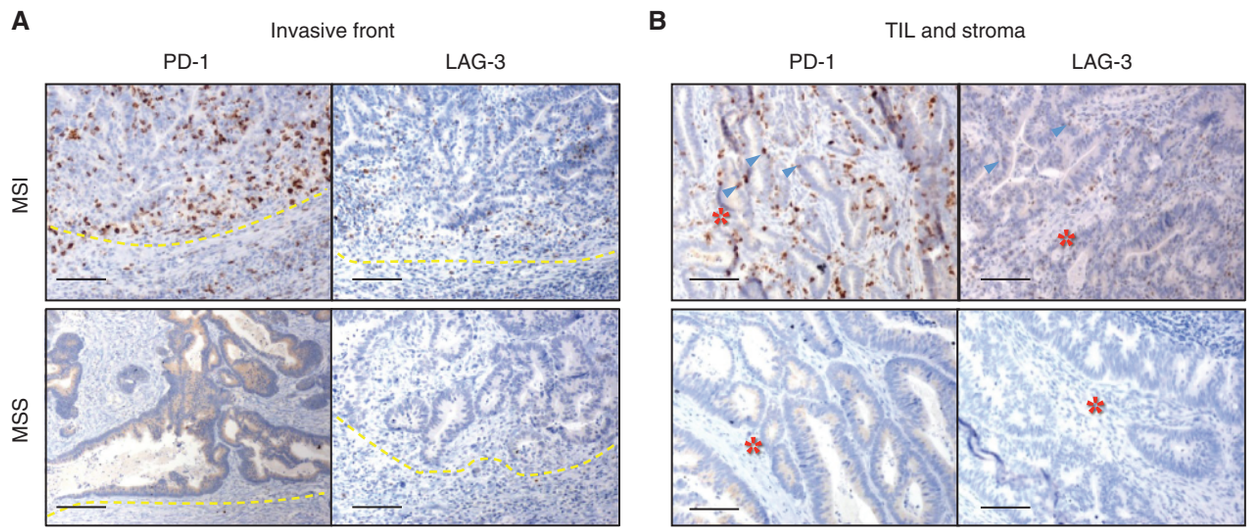

Figure 3. PD-1 and LAG-3 expression in MSI and MSS colorectal cancer specimens. IHC analysis of PD-1 and LAG-3 expression in invasive front (**A**) and TIL/stroma (**B**) areas was performed on formalin-fixed, paraffin-embedded tissue sections of a representative set of MSI (top) and MSS (bottom) colorectal cancer specimens. Magnification, ×20; scale bars, 100 μm; red stars and blue arrows in **B** indicate the tumor stroma and tumor epithelium-infiltrating immune cells, respectively.

a combination of higher immune infiltration and cellular upregulation in MSI compared with MSS tumors.

Because differences in checkpoint expression could have significant implications in defining patient subgroups potentially responsive to checkpoint blockade, we sought to determine whether differences at the RNA level were mirrored at the protein level. Indeed, IHC for both PD-1 and LAG-3 demonstrated robust expression in lymphocytes of MSI tumors, whereas very little was observed in MSS tumors (Fig. 3A and B). The qRT-PCR/LCM analyses shown in Fig. 2 therefore underestimated the differences between MSI and MSS tumors with respect to PD-1 protein surface expression by TIL. Multiparameter flow cytometry of freshly isolated lymphocytes from tumors demonstrated that a large proportion of both $CD4^+$ and $CD8^+$ T cells infiltrating MSI tumors express high levels of PD-1 (Fig. 4A and B). This PD-1^{hi} population was largely absent in MSS tumors (except two MSS specimens, one of which was the highly infiltrated MSS outlier described above) and the normal mucosa adjacent to MSI tumors. The TBET downregulation and PD-1 upregulation by T cells is typically found in chronic viral infection and termed "exhaustion" (18). Because the presence of PD-1^{hi} T-cell infiltrate in MSI tumors is concomitant with the detection of high IFNγ (MFC in Fig. 4C and qRT-PCR in Fig. 2) and high TBET (qRT-PCR in Fig. 2), further investigation should be conducted to determine the coexpression of these molecules at the single cell level and formally rule out the classic "exhaustion" phenotype of these TILs. Of note, the two MSS tumors exhibiting an unusually strong proportion of $PD1^{hi}$ $CD8^+$ T cells (Fig. 4B) were also characterized by a high proportion of IFNγ-producing $CD8^+$ T cells (Supplementary Fig. S3 and data not shown). Our findings suggest that a small proportion of MSS tumors are characterized by the concordant detection of Th1/CTL infiltration and immune checkpoint expression that is found in all MSI tumors.

Finally, we analyzed PD-L1 protein expression by IHC. MSI tumors demonstrated much higher PD-L1 expression than MSS tumors (Fig. 4D). Surprisingly, in contrast to other cancers, such as melanoma, renal cancer, and lung cancer (19), there was virtually no discernable PD-L1 expression on tumor cells of MSI tumors by IHC; rather, costaining with CD163 demonstrated that the majority of PD-L1 expression was by myeloid cells. There were large numbers of PD-$L1^+$ myeloid cells at the invasive front and in the stroma and some were intercalated between epithelial cells in the tumor nests of MSI specimens (Fig. 4D). Histologic scoring of PD-$L1^+$ cells in TIL and the invasive front regions confirmed the high expression of PD-L1 in MSI tumors (Fig. 4E). Omitting the MSS outlier patient (high $CD8^+$ cell infiltration and IFNγ production) that also demonstrated high PD-L1 expression, we found that the difference between MSS and MSI specimens reached statistical significance in the TIL area ($P < 0.05$, Mann–Whitney U test). MFC analysis performed on freshly dissociated MSI tumors confirmed high levels of PD-L1 expression on viable $CD11b^+HLA\text{-}DR^{lo}CD15^-CD14^+CD33^+$ myeloid cells (Fig. 4F). Because most human cancers appear to upregulate PD-L1 as an adaptive response to IFNγ (17), the lack of clear PD-L1 expression on tumor cells in the MSI specimens as assayed by IHC was unexpected, particularly given the high IFNγ level in these tumors. Of note, although PD-L1 was upregulated on a number of both MSI and MSS colon tumor cell lines after incubation with IFNγ, this upregulation was, in general, much less than the one observed in melanoma cell lines (Supplementary Fig. S4). Interestingly, cell lines with the weakest PD-L1 induction also showed weak MHC II induction after IFNγ treatment, suggesting that colon tumors may have relatively dampened STAT1 signaling.

MSI tumors have a much higher mutational load (and thus potentially more neoantigens) than MSS tumors, and

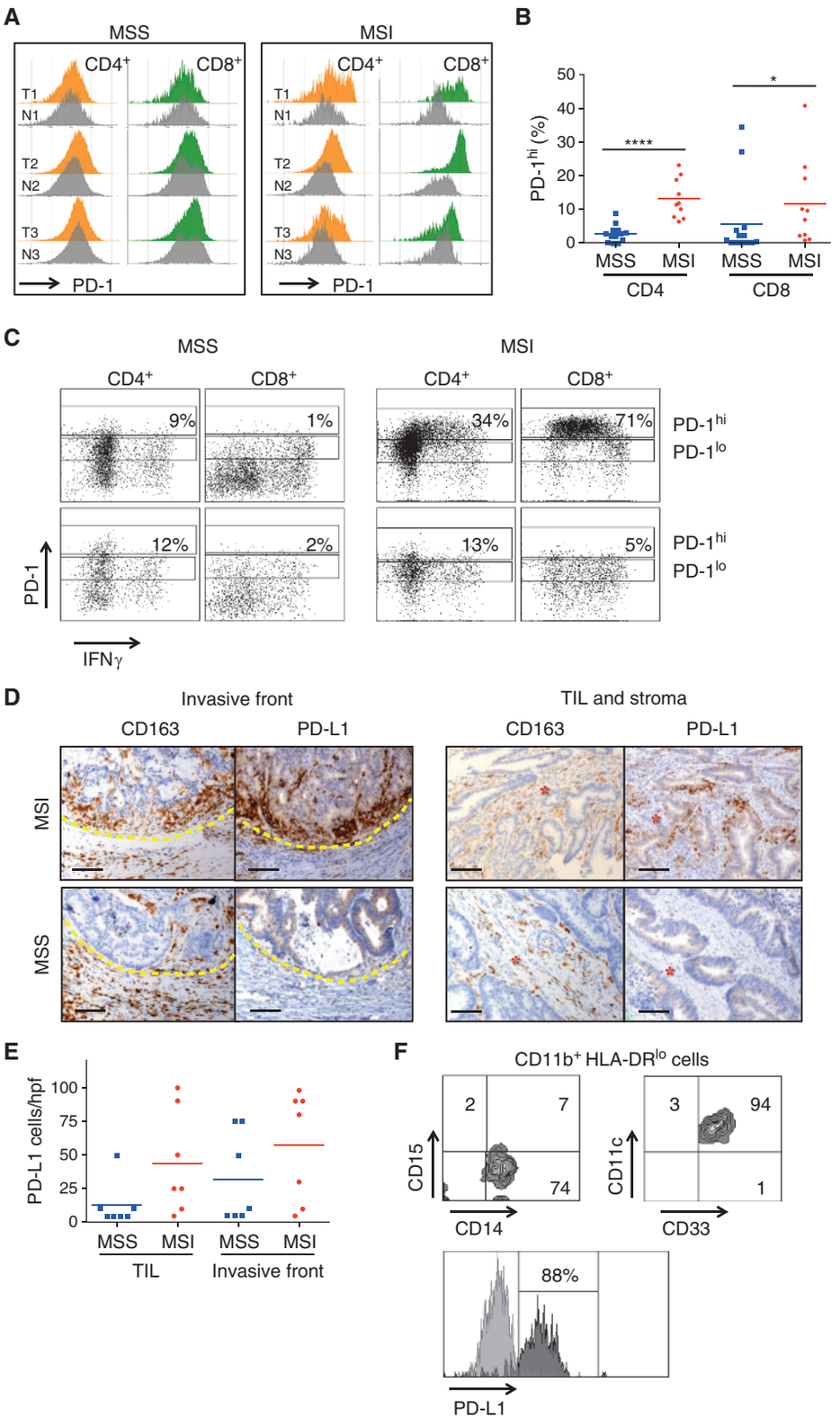

Figure 4. MSI colorectal cancers are characterized by IFNγ-producing PD1^{hi} TIL and PDL-1^{+} tumor-infiltrating myeloid cells. **A,** freshly dissociated MSS and MSI colon tumors (T) as well as patient-matched normal tissue (N) were assessed by MFC for the expression of PD-1 on infiltrating CD4^{+} and CD8^{+} T cells. PD-1 expression in tumor was normalized to the normal tissue run simultaneously and both histograms were aligned to delineate in tumor samples the PD1^{hi} cells when compared with normal tissue. **B,** proportion of PD-1^{hi} CD4^{+} and CD8^{+} cells among CD3^{+} lymphocytes infiltrating MSS (blue squares) and MSI (red circles) specimens. In each group the mean is indicated; *, statistically significant differences between MSS and MSI (*, $P < 0.05$; ****, $P < 0.0001$; nonparametric Mann–Whitney *U* test). **C,** representative ICS for IFNγ production by *in vitro* phorbol-12-myristate-13-acetate/ionomycin–activated T cells (3 hours). The dot plots show the coexpression of PD-1 and IFNγ in CD4^{+} T cells and CD8^{+} T cells in a representative set of MSS (left) and MSI (right) colorectal cancer (top) and patient-matched normal (bottom) specimens. The gates delineate PD1^{hi} and PD1^{lo} cells. **D,** colocalization of CD163 and PD-L1 expression in invasive front (left) and TIL/stroma (right) areas of a representative set of MSS (bottom) and MSI (top) colorectal cancer specimens were assessed by IHC; ×20 magnification. Scale bars, 100 μm. Red stars indicate the tumor stroma. **E,** PD-L1 expression scores in 7 MSS (blue) and 7 MSI (red) colorectal cancer specimens (average of 5 hpf/sample). **F,** MFC analysis of PD-L1 expression on MSI colorectal cancer–infiltrating myeloid cells. Dot plots represent the expression of myeloid-associated markers on CD11b^{+}HLA-DR$^{-/low}$ cells. Infiltrating myeloid cells were characterized as CD15^{-}CD14^{+}CD33^{+}CD11c^{+} cells. PD-L1 expression (dark gray) is overlaid with corresponding isotype control (light gray).

this could be related to the presence of the vigorous immune microenvironment in this genotypic subset of colorectal cancer. We therefore wondered whether the highly infiltrated MSS tumor described above had more mutations than expected for an MSS tumor. To address this question, we performed exome sequencing on the microdissected tumor of this individual. We found only 49 nonsynonymous, somatic mutations in this tumor, a number well within the typical range for MSS colorectal cancer and much less than in MSI tumors (20). In addition, no mutations in *POLE* and *POLD1* genes were identified; tumors with mutations in these genes also contain a high mutational load despite having stable microsatellites (21). Thus, in this individual tumor, the prominent T-cell infiltration was not due to an unusually high mutational load (Supplementary Table S2).

DISCUSSION

Direct analysis of the immune microenvironment of tumors is emerging as the most important means of understanding the relationship between patients' immune systems and their cancer (1). These analyses are bearing fruit in informing prognosis and guiding immunotherapy, particularly using antibody blockade of immune checkpoints. We demonstrate here that the immune microenvironment of DNA repair–deficient MSI colorectal cancer contains a strong Th1 and CTL component not found in the vast majority of DNA repair–sufficient MSS tumors, in keeping with previous reports of high T-cell infiltration in MSI tumors (13–16). More importantly, we address a vexing question in the field: Why are human tumors, which are apparently strongly immunogenic, as judged by histopathologic criteria, not rejected by the host? The numbers of infiltrating activated lymphocytes and CTLs in some tumors are huge, in some cases larger than the number of neoplastic cells. The answer to this question was found through the analysis of immune checkpoints. Multiple key immune-inhibitory ligands, receptors, and metabolic enzymes, including those that are IFNγ inducible (PD-L1, IDO), were highly upregulated in MSI tumors relative to MSS (Fig. 2). We suggest that MSI represents a classic example of adaptive resistance in which an active immune Th1/CTL microenvironment results in compensatory induction of checkpoints that protect the tumor from killing (11).

The mechanistic basis for the link between MSI genetic status and a high Th1/CTL microenvironment in colorectal cancer is not known. However, one important factor may be the increased number of tumor "neoantigens" in DNA repair–deficient tumors created by the high mutational load, typically between 10 and 50 times that of DNA repair–sufficient tumors (14, 16). The notion is that mutation-generated neoantigens are truly tumor specific and may not induce immune tolerance to the same extent as self-antigens, even those upregulated in tumors due to epigenetic dysregulation (22). Ultimately, an altered amino acid due to a coding mutation is only relevant as a tumor neoantigen for T cells if it can be processed and presented on self-MHC. Exomic sequencing and application of a multifactorial algorithm to the mutations in the MSS with an active Th1/Tc1 microenvironment may predict a number of potential neoepitopes capable of being presented on the tumor's HLA class I alleles (23). The multiple variables involved in antigen processing and presentation suggest that although mutational density may correlate with neoantigenicity on a population level, individual tumors with lower mutational load can nonetheless generate good T-cell neoepitopes if the mutations are appropriately positioned. In addition, many other mechanisms besides neoantigenicity (i.e., production of immune regulatory cytokines and chemokines by the tumor and nontransformed stromal cells) likely contribute to the character of the immune microenvironment.

Among the many immune-inhibitory ligand–receptor pairs (checkpoints) and metabolic enzymes discovered to date, CTLA-4, PD-1, PD-L1, LAG-3, and IDO are of particular interest because inhibitory antibodies or drugs (in the case of IDO) are currently in active clinical testing to enhance therapeutic antitumor responses. Of note, all of these were highly elevated in all three compartments (TIL, stroma, and invasive front) of MSI tumors. IHC of PD-1, PD-L1, and LAG-3 confirmed the gene expression findings and demonstrated that MSS tumors and their infiltrating and invasive front lymphocytes (with the exception of the outlier) express very little of these checkpoint molecules. Recent findings point to the elevated expression of these checkpoints in tumors (particularly PD-L1 and IDO) as an adaptive response to cytokines such as IFNγ that are part and parcel of an active intratumoral immune response (24, 25). This mechanism appears to be operative in MSI tumors. What is strikingly different in MSI colorectal cancer relative to melanoma, renal, or lung cancer is that there is little PD-L1 expressed by tumor cells; rather it is expressed predominantly by infiltrating myeloid cells. The modest upregulation of PD-L1 by colorectal cancer cell lines in response to *in vitro* incubation with IFNγ suggests that adaptive PD-L1 expression in colorectal cancer is predominantly at the level of infiltrating myeloid cells, though low levels of PD-L1 could be expressed by tumor cells *in situ* that are below the detection level of IHC. Regardless, a very important prediction of our findings on differential expression of immune-inhibitory ligands, receptors, and metabolic enzymes is that MSI tumors will respond to checkpoint blockade with agents such as anti–PD-1 or anti–PD-L1 antibodies, whereas MSS tumors will be much less responsive. Indeed, based on these findings, two clinical trials testing anti–PD-1 antibodies in patients selected based on MSI have been initiated (NCT01876511 and NCT02060188).

METHODS

Patient Selection, Tumor Samples, and Cell Lines

Tumor tissues were collected at the Johns Hopkins Hospital (Baltimore, MD) from patients with primary sporadic colorectal cancer and free of prior chemotherapy. Demographic, pathologic [tumor location and tumor–node–metastasis (TNM) grade] and genetic status are detailed in Supplementary Table S1. This study was approved by the Johns Hopkins Institutional Review Board. All samples were obtained in accordance with the Health Insurance and Accountability Act.

Assessment of MSI was done using the length of a panel of microsatellite markers in the tumor and a normal reference (either normal mucosa or germline) by using fragment analysis of PCR products labeled with fluorescent dyes. Fragment analysis determined the expression level of the proteins in charge of maintaining the integrity of microsatellite tracts. Differences in the length of two or more markers (the standard Bethesda panel uses five markers) were

indicative of MSI status. Eleven patients tested as MSI positive and 14 patients as MSS (Supplementary Table S1).

Analysis of mutations on the MSS outlier sample was performed using DNA exomic sequencing from formalin-fixed, paraffin-embedded (FFPE) tissues. Identification of tumor-specific mutations involved comparison with normal matched cells derived from FFPE sections that contained no tumor. Genomic DNA libraries were prepared following Illumina's suggested protocol with small modification. Briefly, the ends of sheared genomic DNA fragments are blunted and Illumina adaptors are ligated. The fragment library was amplified by 15 cycles of PCR. Human exome capture is performed following a modified protocol from Agilent's SureSelect Paired-End Version 2.0 Human Exome Kit (Agilent). The genomic library is hybridized to the SureSelect probes. After washes, the genomic regions captured by the probes are eluted. The captured region covers 38 Mb of exomic sequences. Following PCR amplification of six cycles, the library is hybridized to an Illumina flow cell and eventually sequenced according to Illumina's protocols. Mismatched bases were identified as a mutation based on rigorous criteria described previously. Mutations were further confirmed to not be variants present in the normal population according to the NCBI Single Nucleotide Polymorphism Database.

For analysis of cell lines, three microsatellite instable (SW48, HCT116, and DLD1) and three chromosomal instable (HT29, Caco-2, and SW480) human colorectal cancer cell lines were used. These cell lines were obtained from the Genetic Resources Core Facility (GRCF), Institute of Genetic Medicine, Johns Hopkins School of Medicine, which purchased these cells from the authenticated ATCC repository. The cell lines were maintained in culture in 10% fetal calf serum DMEM supplemented with L-glutamine, nonessential amino acids, sodium pyruvate, and antibiotics.

Immunohistochemistry

FFPE specimens were cut into 5-μm sections and mounted on glass slides. For each specimen, CD3 (clone PS1; Leica Biosystems), CD4 (clone Sp35; Ventana), CD8 (clone C8144B; Cell Marque), Foxp3 (236A/E7; Abcam), and CD163 (clone Novacastra10D6; Leica Biosystems) stainings were performed according to standard protocols. IHC for PD-L1 (clone 5H1) and PD-1 (clone M3) stainings was performed according to a protocol previously reported (24). Positive cells were counted in 5 hpf (0.028 mm/hpf; Olympus BX41) by two blinded pathologists (R.A. Anders and M. Cruise) in three distinct tumor areas denominated TIL, tumor stroma, and invasive front. LAG3 IHC was performed using clone 17B4 (LS Bio).

Laser Capture Microdissection and TaqMan Quantitative RT-PCR

FFPE and hematoxylin and eosin–stained tissue sections (5 μm) were used for the LCM procedure using the Leica LMD 7000 system. For each patient, tissues were microdissected from the three previously defined areas and directly collected in tissue lysis buffer for RNA extraction. RNA was isolated following the manufacturer's instructions (High Pure Paraffin Kit; Roche). RNA was converted to cDNA using the High-Capacity RNA-to-cDNA Kit (Life Technologies) and a step of preamplification was first done using a pool of primers and a preamplification master mix kit (Life Technologies), followed by TaqMan RT-PCR (list of primers in Supplementary Table S3). Data are expressed as $2^{-\Delta Ct}$, where ΔC_t represents $C_{t\ gene} - C_{t\ ctrl}$. For our calculation, $C_{t\ ctrl}$ is the average of C_t for two ubiquitous genes (*GAPDH* and *GUSB*). When undetectable, a value of 40 was assigned as C_t.

Tumor Processing and Flow Cytometry

Tumor specimens were collected and freshly dissociated using enzymatic cocktail (0.1% DNaseI and Liberase 400 μ/mL; Roche). Leukocytes were enriched by Percoll density gradient (GE Healthcare) and cells were banked in liquid nitrogen until further analysis. MFC was performed with a LSRII cytometer (BD Biosciences). Samples were stained with anti-CD45 (2D1; BD Biosciences) anti-CD3 (UCHT1; BD Biosciences), anti-CD4 (OKT4; BD Biosciences), anti-CD8 (RPA-T8; BD Biosciences), anti–PD-1 (EH12.1; BD Biosciences), and anti-FOXP3 (259D/C7; BD Biosciences). Cytokine intracellular staining (ICS) for IFNγ (B27; BD Biosciences) and IL17 (SCPL1362; BD Biosciences) was performed following 3-hour *in vitro* stimulation in the presence of stimulation cocktail (phorbol-12-myristate-13-acetate + ionomycin; eBioscience) and GolgiStop (Monensin; BD Biosciences) according to the manufacturer's instructions. Data were analyzed using DIVA 6.1 Software (BD Biosciences). Myeloid cells were stained using anti-CD45, anti-CD11b (ICRF44; BD Biosciences), anti-DR (G46.6; BD Biosciences), anti-CD15 (HI98; BD Biosciences), anti-CD14 (M5E2; BD Biosciences), anti-CD33 (WM53; BD Biosciences), anti-CD11c (B-Ly6; BD Biosciences), and anti–PD-L1 (29E.2A3; BioLegend). Cell lines were cultured for 3 days in the presence or absence of IFNγ (500 IU/mL). Cells were stained with DR and B7-H1/PD-L1 mAb before analysis by flow cytometry.

Statistical Analysis

IHC scoring in each of the three histologic areas (i.e., TIL, stroma, and invasive front) and MFC data were summarized using scatter plots and compared between MSI and MSS patients using means and the nonparametric Mann–Whitney *U* test. For the gene expression analysis, scatter plots and geometric means were used to characterize MSI/MSS patient groups for each of the three locations. Genes were grouped by lineage and/or function (Th1/Tc1, CTL, Th17, Treg, proinflammation, and metabolism), and to distinguish which groups of genes were differentially expressed on the basis of MSS/MSI status, a resampling-based permutation test was conducted on the basis of the maximum Wilcoxon–Mann–Whitney test statistic within the gene group. Individual gene expression was also compared across MSI/MSS status using the Wilcoxon–Mann–Whitney test. All tests are descriptive and no multiplicity adjustment was considered. Statistical analysis was performed using the R statistical package (version 2.15.1).

Disclosure of Potential Conflicts of Interest

J.M. Taube reports receiving a commercial research grant from Bristol-Myers Squibb and is a consultant/advisory board member for the same. K.W. Kinzler has ownership interest (including patents) in PGDx and is a consultant/advisory board member for Symex-Inostics. B. Vogelstein has ownership interest (including patents) in PGDx and PapGene, Inc.; is a consultant/advisory board member for Symex-Inostics; and has licensed inventions through Johns Hopkins University. R.A. Anders reports receiving a commercial research grant from Bristol-Myers Squibb. D.M. Pardoll is a consultant/advisory board member for Aduro, ImmuneXcite, Medimmune, and Bristol-Myers Squibb. No potential conflicts of interest were disclosed by the other authors.

Authors' Contributions

Conception and design: N.J. Llosa, M. Cruise, E.M. Hechenbleikner, N. Papadopoulos, K.W. Kinzler, B. Vogelstein, C.L. Sears, R.A. Anders, F. Housseau

Development of methodology: N.J. Llosa, M. Cruise, J.M. Taube, K.W. Kinzler, R.A. Anders, F. Housseau

Acquisition of data (provided animals, acquired and managed patients, provided facilities, etc.): N.J. Llosa, M. Cruise, A. Tam, E.C. Wick, E.M. Hechenbleikner, J.M. Taube, H. Fan, M. Zhang, N. Papadopoulos, K.W. Kinzler, C.L. Sears, R.A. Anders, F. Housseau

Analysis and interpretation of data (e.g., statistical analysis, biostatistics, computational analysis): N.J. Llosa, A. Tam, E.M. Hechenbleikner, J.M. Taube, R.L. Blosser, H. Wang, B.S. Luber, N. Papadopoulos, K.W. Kinzler, C.L. Sears, R.A. Anders, F. Housseau

Writing, review, and/or revision of the manuscript: N.J. Llosa, M. Cruise, E.M. Hechenbleikner, J.M. Taube, H. Wang, B.S. Luber,

N. Papadopoulos, K.W. Kinzler, B. Vogelstein, C.L. Sears, R.A. Anders, D.M. Pardoll, F. Housseau

Administrative, technical, or material support (i.e., reporting or organizing data, constructing databases): A. Tam, E.C. Wick, E.M. Hechenbleikner, K.W. Kinzler, F. Housseau

Study supervision: N.J. Llosa, C.L. Sears, F. Housseau

Acknowledgments

The authors thank K. Judge and C. Blair for excellent management and coordination of colorectal cancer patient recruitment and specimen banking. The authors acknowledge Robert Scharpf (Department of Biostatistics, Johns Hopkins University School of Medicine, Baltimore, Maryland) for his helpful expertise in genomic data analysis.

Grant Support

This work was supported by the NIH through P50 CA062924 (GI SPORE to F. Housseau), RO1 CA151393 (to C.L. Sears and D.M. Pardoll), K08 DK087856 (to E.C. Wick), 5T32CA126607-05 (to E.M. Hechenbleikner), P30 DK089502 (GI Core), and P30 CA006973 (Sidney Kimmel Comprehensive Cancer Center core). Additional support was provided by GSRRIG-015 (American Society of Colon and Rectal Surgeons, to E.M. Hechenbleikner), the Mérieux Foundation (to C.L. Sears and D.M. Pardoll), Stand Up To Cancer–Cancer Research Institute Cancer Immunology Dream Team Translational Research Grant SU2C-AACR-DT1012 (Stand Up To Cancer is a program of the Entertainment Industry Foundation administered by the American Association for Cancer Research), a Melanoma Research Alliance award (to D.M. Pardoll), the Commonwealth Foundation (to K.W. Kinzler, N. Papadopoulos, and B. Vogelstein), and The Virginia and D.K. Ludwig Fund for Cancer Research and the Ludwig Institute (to K.W. Kinzler and B. Vogelstein).

The costs of publication of this article were defrayed in part by the payment of page charges. This article must therefore be hereby marked *advertisement* in accordance with 18 U.S.C. Section 1734 solely to indicate this fact.

Received August 6, 2014; revised October 20, 2014; accepted October 23, 2014; published OnlineFirst October 30, 2014.

REFERENCES

1. Fridman WH, Pages F, Sautes-Fridman C, Galon J. The immune contexture in human tumours: impact on clinical outcome. Nat Rev Cancer 2012;12:298–306.
2. Galon J, Costes A, Sanchez-Cabo F, Kirilovsky A, Mlecnik B, Lagorce-Pages C, et al. Type, density, and location of immune cells within human colorectal tumors predict clinical outcome. Science 2006;313:1960–4.
3. Tosolini M, Kirilovsky A, Mlecnik B, Fredriksen T, Mauger S, Bindea G, et al. Clinical impact of different classes of infiltrating T cytotoxic and helper cells (Th1, th2, treg, th17) in patients with colorectal cancer. Cancer Res 2011;71:1263–71.
4. Shankaran V, Ikeda H, Bruce AT, White JM, Swanson PE, Old LJ, et al. IFNgamma and lymphocytes prevent primary tumour development and shape tumour immunogenicity. Nature 2001;410:1107–11.
5. Wilke CM, Kryczek I, Wei S, Zhao E, Wu K, Wang G, et al. Th17 cells in cancer: help or hindrance? Carcinogenesis 2011;32:643–9.
6. Topalian SL, Hodi FS, Brahmer JR, Gettinger SN, Smith DC, McDermott DF, et al. Safety, activity, and immune correlates of anti-PD-1 antibody in cancer. N Engl J Med 2012;366:2443–54.
7. Brahmer JR, Tykodi SS, Chow LQ, Hwu WJ, Topalian SL, Hwu P, et al. Safety and activity of anti-PD-L1 antibody in patients with advanced cancer. N Engl J Med 2012;366:2455–65.
8. Topalian SL, Sznol M, McDermott DF, Kluger HM, Carvajal RD, Sharfman WH, et al. Survival, durable tumor remission, and long-term safety in patients with advanced melanoma receiving nivolumab. J Clin Oncol 2014;32:1020–30.
9. Hamid O, Robert C, Daud A, Hodi FS, Hwu WJ, Kefford R, et al. Safety and tumor responses with lambrolizumab (anti-PD-1) in melanoma. N Engl J Med 2013;369:134–44.
10. Hirano F, Kaneko K, Tamura H, Dong H, Wang S, Ichikawa M, et al. Blockade of B7-H1 and PD-1 by monoclonal antibodies potentiates cancer therapeutic immunity. Cancer Res 2005;65:1089–96.
11. Pardoll DM. The blockade of immune checkpoints in cancer immunotherapy. Nat Rev Cancer 2012;12:252–64.
12. Boland CR, Goel A. Microsatellite instability in colorectal cancer. Gastroenterology 2010;138:2073–87.
13. Kim H, Jen J, Vogelstein B, Hamilton SR. Clinical and pathological characteristics of sporadic colorectal carcinomas with DNA replication errors in microsatellite sequences. Am J Pathol 1994;145:148–56.
14. Smyrk TC, Watson P, Kaul K, Lynch HT. Tumor-infiltrating lymphocytes are a marker for microsatellite instability in colorectal carcinoma. Cancer 2001;91:2417–22.
15. Dolcetti R, Viel A, Doglioni C, Russo A, Guidoboni M, Capozzi E, et al. High prevalence of activated intraepithelial cytotoxic T lymphocytes and increased neoplastic cell apoptosis in colorectal carcinomas with microsatellite instability. Am J Pathol 1999;154:1805–13.
16. Phillips SM, Banerjea A, Feakins R, Li SR, Bustin SA, Dorudi S. Tumour-infiltrating lymphocytes in colorectal cancer with microsatellite instability are activated and cytotoxic. Br J Surg 2004;91:469–75.
17. Dong H, Strome SE, Salomao DR, Tamura H, Hirano F, Flies DB, et al. Tumor-associated B7-H1 promotes T-cell apoptosis: a potential mechanism of immune evasion. Nat Med 2002;8:793–800.
18. Kao C, Oestreich KJ, Paley MA, Crawford A, Angelosanto JM, Ali MA, et al. Transcription factor T-bet represses expression of the inhibitory receptor PD-1 and sustains virus-specific $CD8^+$ T cell responses during chronic infection. Nat Immunol 2011;12:663–71.
19. Taube JM, Klein A, Brahmer JR, Xu H, Pan X, Kim JH, et al. Association of PD-1, PD-1 ligands, and other features of the tumor immune microenvironment with response to anti-PD-1 therapy. Clin Cancer Res 2014;20:5064–74.
20. Vogelstein B, Papadopoulos N, Velculescu VE, Zhou S, Diaz LA Jr, Kinzler KW. Cancer genome landscapes. Science 2013;339:1546–58.
21. Palles C, Cazier JB, Howarth KM, Domingo E, Jones AM, Broderick P, et al. Germline mutations affecting the proofreading domains of POLE and POLD1 predispose to colorectal adenomas and carcinomas. Nat Genet 2013;45:136–44.
22. Segal NH, Parsons DW, Peggs KS, Velculescu V, Kinzler KW, Vogelstein B, et al. Epitope landscape in breast and colorectal cancer. Cancer Res 2008;68:889–92.
23. van Rooij N, van Buuren MM, Philips D, Velds A, Toebes M, Heemskerk B, et al. Tumor exome analysis reveals neoantigen-specific T-cell reactivity in an ipilimumab-responsive melanoma. J Clin Oncol 2013;31:e439–42.
24. Taube JM, Anders RA, Young GD, Xu H, Sharma R, McMiller TL, et al. Colocalization of inflammatory response with B7-h1 expression in human melanocytic lesions supports an adaptive resistance mechanism of immune escape. Sci Transl Med 2012;4:127ra37.
25. Spranger S, Spaapen RM, Zha Y, Williams J, Meng Y, Ha TT, et al. Up-regulation of PD-L1, IDO, and T(regs) in the melanoma tumor microenvironment is driven by CD8(+) T cells. Sci Transl Med 2013;5:200ra116.